

*This paper was not presented at the conference:*

**Title:** Multispectral Plasmonic Structures Using Native Aluminum Oxide and Aluminum  
**Authors:** sencer ayas, Gokhan Bakan, and Aykutlu Dana  
**Event Name:** CLEO: Applications and Technology  
**Year:** 2017

# Multispectral Plasmonic Structures Using Native Aluminum Oxide and Aluminum

Sencer Ayas<sup>[\*a,b]</sup>, Gokhan Bakan<sup>[a,c]</sup> and Aykutlu Dana<sup>[a]</sup>

<sup>a</sup>UNAM, Institute of Materials Science and Nanotechnology, Bilkent University, Ankara, 06800, Turkey.

<sup>b</sup>Department of Radiology, Canary Center at Stanford for Cancer Early Detection, Stanford University School of Medicine

<sup>c</sup>Department of Electrical and Electronics Engineering, Atilim University, Ankara, 06830, Turkey

\*sencerayas@gmail.com

**Abstract:** We report the use of native aluminum oxide to fabricate periodic metal-insulator-metal resonators with simultaneous resonances in the visible and IR wavelengths. The cavity size is in the order of  $\lambda^3/25000$  in the NIR .

**OCIS codes:** (240.6680) Surface plasmons; (160.3918) Metamaterials

## 1. Introduction

Recent advancements in plasmonics and nanophotonics enabled the development of novel plasmonic materials for UV and IR wavelengths[1]–[4]. Au and Ag are the most common materials to study plasmon-enhanced optical phenomena such as surface enhanced raman spectroscopy (SERS), surface enhanced infrared absorption (SEIRA) spectroscopy and plasmon enhanced harmonic generation[5], [6]. Although Au has a band transition around 500nm which makes it less desirable material for visible and UV plasmonic applications. Being chemically inert material and tailorable molecule binding properties make Au a widely used material for sensing applications.[7] Ag is known as the optimal plasmonic material due to its low loss in the visible wavelengths. Since Ag is prone to oxidation and atmospheric sulfur contamination, it is not preferred for applications that require durability.[8] Al, on the other hand, is known as a durable metal under atmosphere owing to its naturally formed thin native oxide layer[9]. Despite its use as interconnects in semiconductor fabrication processes, Al is not widely used material in plasmonic applications due to its high optical losses in the visible and IR regimes. Yet, Al is used for deep-UV and UV applications owing to its high plasma frequency[10]. Although, various plasmonic surfaces were realized using Al recently, the effect of native oxide layer on the optical response of these fabricated surfaces has not been analyzed deeply. In this work, we used the native  $\text{Al}_2\text{O}_3$  and Al for the fabrication of metal-insulator-metal (MIM) plasmonic resonators[11].

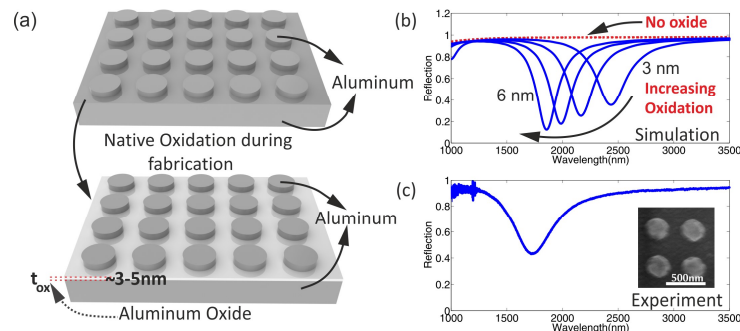


Fig 1. (a) Schematic of formation of native oxide MIM surfaces during fabrication process. (b) Simulated reflectance spectrum of MIM structures for various  $\text{Al}_2\text{O}_3$  thicknesses. (c) Experimental reflection spectra of the fabricated nanodisc structure. Diameter and period of the discs are 250nm and 400nm, respectively. (Inset) SEM image of the nanodisc array.

## 2. Results

In Fig.1(a), the schematic of fabricated Al plasmonic surfaces is shown. MIM structures are formed naturally where the need for the deposition of insulator layer is eliminated due to native  $\text{Al}_2\text{O}_3$  layer. Typically, fabrication process of native oxide based MIM structures requires multiple metal deposition processes. After depositing the first Al layer, the vacuum is broken for PMMA coating and e-beam lithography, which is accompanied by formation of a thin layer of  $\text{Al}_2\text{O}_3$  on the surface of Al. After metal deposition and lift-off processes, MIM structures are formed. fabricated structures are characterized by a Fourier Transform Infrared Reflection (FTIR) microscope system equipped with a 15x Cassegrain objective. A knife edge aperture is used to limit measurement area to regions containing lithographically defined structures ( $100\mu\text{m} \times 100\mu\text{m}$ ). Simulated and reflected spectra are shown in Fig.1(b). In the reflection spectra resonances in the NIR wavelengths are observed. Without the oxide layer, no

resonance is observed as shown in Fig.1(b). However, as we include oxide layer NIR resonances are emerged. As the thickness of oxide increases, this resonance blue-shifts. NIR resonance in the measured reflection spectrum proves the resonance is due to presence of native oxide layer as shown in fig.2(b). The size of the cavity is in the order of  $\lambda^3/25000$  by assuming a 5nm native  $\text{Al}_2\text{O}_3$  thickness.

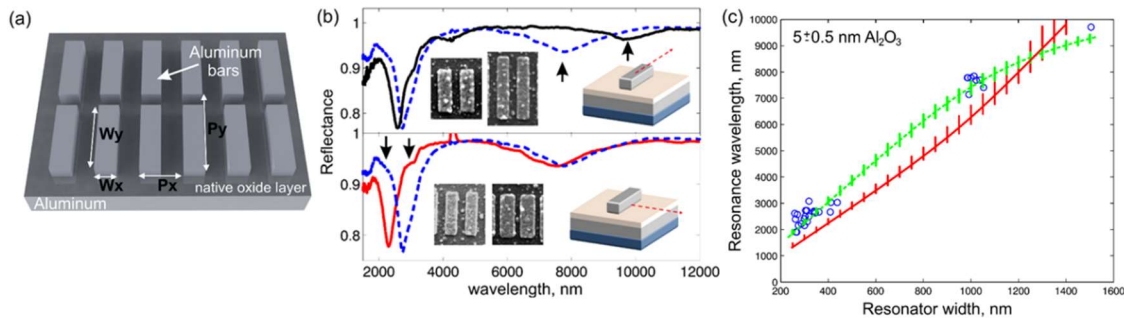


Fig 2. (a) Schematic of asymmetric of native oxide MIM. (b) Tuning resonance wavelength of asymmetric of native oxide MIM by changing width or length of bars (c) Modelling of resonance wavelengths using Fabry-Perot model.

To estimate the thickness of native  $\text{Al}_2\text{O}_3$ , we have fabricated asymmetric bar structures as shown in Fig. 2. The resonance wavelength is tuned by changing either width or length of the structures as shown in Fig. 2(b). By solving the characteristic equation given by (1), we estimated  $5 \pm 0.5$  nm native  $\text{Al}_2\text{O}_3$  as shown in Fig. 2(c) where  $W_{S,L}$  are the widths long the short and long axes,  $n_{\text{eff}}$  is the effective refractive index of the propagating mode and  $\varphi_{S,L}$  is the phase term due to the reflection from the terminations.

$$W_{S,L} \frac{2\pi}{\lambda} n_{\text{eff}} = \pi - \varphi_{S,L} \quad (1)$$

### 3. Conclusion

In conclusion, for the first time we have demonstrated the use of native  $\text{Al}_2\text{O}_3$  and Al to fabricate MIM resonators. The use of native  $\text{Al}_2\text{O}_3$  eliminates the deposition of insulator layer. The resonance wavelength can be easily tuned by changing the thickness of native  $\text{Al}_2\text{O}_3$  layer by exposure time of Al surfaces to air. Our results can help to develop more complex Al based plasmonic surfaces in the visible and IR wavelengths for sensing, energy and metamaterial applications.

### 4. References

- [1] R. Alaei et al., "Deep-subwavelength plasmonic nanoresonators exploiting extreme coupling.," *Nano Lett.*, 13, 8, 3482–6, Aug. 2013.
- [2] A. Boltasseva and H. a Atwater, "Materials science. Low-loss plasmonic metamaterials.," *Science*, 331, 6015, 290–1, 2011.
- [3] J. B. Khurgin and A. Boltasseva, "Reflecting upon the losses in plasmonics and metamaterials.," *MRS Bull.*, 37, 08, 768–779, 2012.
- [4] G. V Naik et al., "Demonstration of Al:ZnO as a plasmonic component for near-infrared metamaterials.," *Proc. Natl. Acad. Sci. U. S. A.*, 109, 23, 8834–8, 2012.
- [5] K. Chen, R. Adato, and H. Altug, "Dual-Band Perfect Absorber for Infrared Spectroscopy.," *ACS Nano*, 6, 9, 7998–8006, 2012.
- [6] S. Palomba, S. Zhang, Y. Park, G. Bartal, X. Yin, and X. Zhang, "Optical negative refraction by four-wave mixing in thin metallic nanostructures.," *Nat. Mater.*, 11, 1, 34–8, 2012.
- [7] P. R. West, S. Ishii, G. V. Naik, N. K. Emani, V. M. Shalaev, and a. Boltasseva, "Searching for better plasmonic materials.," *Laser Photon. Rev.*, 4, 6, 795–808, 2010.
- [8] J. C. Reed, H. Zhu, A. Y. Zhu, C. Li, and E. Cubukcu, "Graphene-enabled silver nanoantenna sensors.," *Nano Lett.*, 12, 8, 2012.
- [9] M. W. Knight et al., "Aluminum for plasmonics.," *ACS Nano*, 8, 1, 834–40, 2014.
- [10] S. K. Jha, Z. Ahmed, M. Agio, Y. Ekinci, and J. F. Löffler, "Deep-Ultraviolet Surface-Enhanced Resonance Raman Scattering of Adenine on Aluminum Nanoparticle Arrays.," *J. Am. Chem. Soc.*, 134, 4, 1966–1969, 2012.
- [11] S. Ayas, A. E. Topal, A. Cupallari, H. Guner, G. Bakan, and A. Dana, "Exploiting Native  $\text{Al}_2\text{O}_3$  for Multispectral Aluminum Plasmonics.," *ACS Photonics*, 2014